J Mol Model (2002) 8:173–183
DOI 10.1007/s00894-002-0082-0

ORIGINAL PAPER

**Federico Iribarne · Margot Paulino · Sara Aguilera
Miguel Murphy · Orlando Tapia**

# Docking and molecular dynamics studies at trypanothione reductase and glutathione reductase active sites

Received: 9 January 2002 / Accepted: 3 April 2002 / Published online: 22 May 2002


**Abstract** A theoretical docking study on the active sites of trypanothione reductase (TR) and glutathione reductase (GR) with the corresponding natural substrates, trypanothione disulfide ($T[S]_2$) and glutathione disulfide (GSSG), is reported. Molecular dynamics simulations were carried out in order to check the robustness of the docking results. The energetic results are in agreement with previous experimental findings and show the crossed complexes have lower stabilization energies than the natural ones. To test DOCK3.5, four nitro furanic compounds, previously designed as potentially active anti-chagasic molecules, were docked at the GR and TR active sites with the DOCK3.5 procedure. A good correlation was found between differential inhibitory activity and relative interaction energy (affinity). The results provide a validation test for the use of DOCK3.5 in connection with the design of anti-chagasic drugs.

**Keywords** Chagas' disease · Computer design · Theoretical docking · Molecular dynamics · Selective inhibitors

## Introduction

Trypanosomatids, protozoa belonging to the order Kinetoplastida, suborder Trypanosomatina, are the causative agents of a number of infectious diseases that pose serious medical and economic problems for many millions of people. In particular, Chagas' disease, caused by *Trypanosoma cruzi* (*T. cruzi*), is very prevalent in Latin America. [1] Although these infectious diseases have been the targets of extensive scientific research, the c urrent therapies for trypanosomal infection are far from adequate; the low efficacy and high toxicity of current drugs help explain this failure. [2] The situation is aggravated by the ability of trypanosomatids to develop drug resistance rapidly. Therefore, there is a great need for new and improved drugs.

One possible approach to the problem is knowledge based drug development. [3, 4, 5] In effect, after identification and structure and function characterization of a given metabolic pathway or enzyme, the resulting information can be utilized to search for appropriate drugs, acting, for instance, as enzyme inhibitors. In this respect, the catalytic enzyme couple glutathione/trypanothione reductase offers one possible target for therapy development. Glutathione reductase (GR) in humans and trypanothione reductase (TR) in trypanosomatids ensure high thiol levels inside the cells by acting specifically on their cognate disulfide substrates, GSSG (L-γ-glutamyl-L-cysteinylglycine) and $T[S]_2$ ($N^1$,$N^8$-bis(glutathionyl) spermidine), respectively. The structural formulae of GSSG and $T[S]_2$ are detailed in Scheme 1. GR catalyzes the NADPH-dependent reduction of GSSG to yield the thiol form, GSH. It is this species that plays a significant role in cell metabolism. [6] Among its numerous functions, the scavenging of free radical derivatives stands out. TR, in trypanosomatids, acts in a similar fashion to its mammal counterpart, converting $T[S]_2$ to the dithiol form, $T[SH]_2$, again using NADPH as coenzyme. Trypanosomes contain low levels of GSH, but no GR. Rather, $T[SH]_2$ helps reduce GSSG by means of thiol–disulfide exchange. [7] In this way, GSH is also responsible for the neutralization of highly reactive species in trypanosomatids. Thus, selective inhibition of TR has been considered by many authors to be a possible solution.

F. Iribarne · M. Paulino
Lab. de Modelado Biomolecular,
Depto de Quimico-Física y Matemáticas, Facultad de Química,
Universidad de la República,
Gral. Flores 2124, C.C. 1157, Montevideo, Uruguay

S. Aguilera · M. Murphy
Lab. de Cristalografía Macromolecular,
Depto. de Física, Facultad de Ciencias,
Universidad Católica del Nortem,
Avda. Angamos 0610, C.C. 1280, Antofagasta, Chile

O. Tapia (✉)
Department of Physical Chemistry, Uppsala University,
P.O. Box 532, 751 21 Uppsala, Sweden
e-mail: orlando.tapia@fki.uu.se

I

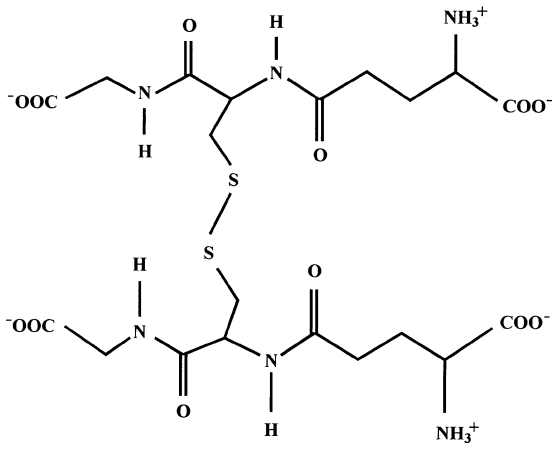

II

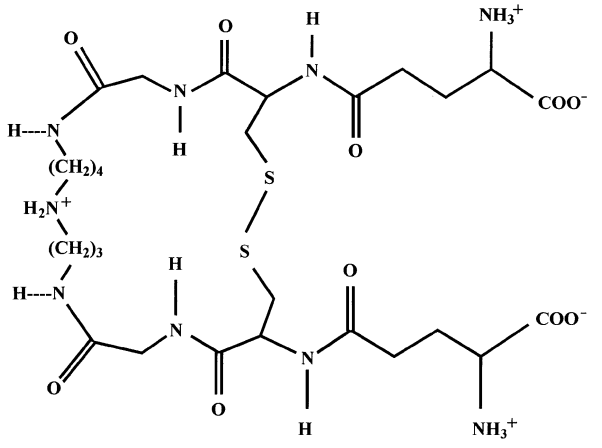

**Scheme 1** Molecular formulae for **I**: glutathione disulfide (GSSG) and **II**: trypanothione disulfide ($T[S]_2$)

Over the past few years, a great deal of work has been devoted to the elucidation of the three-dimensional structures of GR and TR. As a result, the crystal structures from a variety of sources, including the complex with the substrate, are now available. [8, 9, 10, 11, 12, 13] GR and TR belong to the family of flavin-containing disulfide oxido-reductases. They are active as homo-dimers of about 52 kDa per subunit mass and display an overall 40% sequence homology. [14, 15, 16, 17, 18] The catalytic site is rather complex, comprising two separate regions, i.e., the NADP site (N-site) and the active site (G-site), connected to each other by the flavin ring of FAD and a redox active disulfide bridge. Besides, the dimer interface region defines a putative binding site known as the allosteric site. There is evidence that suitable ligands, such as menadione (2-methyl-1,4-naphtoquinone), bound at this site, can elicit molecular perturbations capable of being transmitted onto the catalytic region. [19] This site is not studied here.

The structural catalytic elements in GR and TR are conserved: namely, the redox active isoalloxazine ring of FAD, a disulfide bridge, and two couples of proton relay residues at the G-site (active site) and N-site (NADP site), respectively. The proton relay function acts during the electron transfer step. [20, 21] The electrons from the nicotinamide are thought to flow successively along the isoalloxazine and the disulfide bridge, finally reducing the substrate disulfide. [20, 21] The crucial feature in relation to therapeutic strategies is the fact that each enzyme is specific for its cognate substrate; the crossed-complexes, GR–$T[S]_2$ and TR–GSSG, have proven to be non-catalytic. [22] This supports the possibility for a selective inhibition of the parasite enzyme, thus leaving the host GR unaffected. Given the key role of TR in relation to the survival of the parasite, [23, 24, 25] it is clear that the selective inactivation of the enzyme would render the trypanosome susceptible to massive oxidative stress resulting in rapid cellular decay. Hence, TR appears to be an optimal target for rationally based drug design.

In the past, a fair number of candidates for selective inhibition have been proposed. [26, 27, 28, 29, 30, 31, 32, 33] In particular, it is well known that nitrofuran compounds are active as enzyme inhibitors of trypanothione reductase. In fact, one such compound, Nifurtimox, has been widely used in the treatment of acute Chagas' disease. Nevertheless, a truly selective inhibitor of the parasite enzyme has turned out to be elusive.

It is widely accepted that productive binding, usually implying a molding work of the substrate, is a key step in enzyme catalyzed reactions. [34] This process has to be fulfilled before the actual chemical steps at the active site take place. In this sense, ligands (e.g. inhibitors) that are able to occupy the active site readily at low molding intramolecular energy expenses, would form the most stable complexes with the catalytic receptor and eventually would undergo chemical reaction. [34and references therein] Therefore, an accurate energy measure of the binding step is desirable if one is to assess the relative inhibitory capacity of a given set of molecules towards particular enzyme or receptor sites.

Theoretical docking procedures [35, 36, 37] are suitable tools to adjust ligands at target sites and to estimate interaction energy (affinity) of the binding step by means of rigid energy minimization methods of the molecular interactions involved. Alternatively, one can resort to more elaborated approaches such as molecular dynamics, [38, 39] which provide more accurate and detailed energetic measurements on ligand–receptor molecular interactions, as solvation effects and accessible configurational space related components can be taken into account. From these data, an affinity, obtained as interaction energy, can easily be extracted.

Here, we present a theoretical docking study on the substrates GSSG and $T[S]_2$ at the active sites of glutathione reductase and trypanothione reductase in order to provide structural and energetic clues on the above mentioned ligand specificity. Four different complexes were obtained, namely, GR–GSSG and TR–$T[S]_2$ and the crossed complexes GR–$T[S]_2$ and TR–GSSG. To evaluate the robustness of the docking results, molecular dynamics simulations are performed on the ligand–enzyme complexes. A word of caution is necessary. The

purpose in using MD calculations is to get a measure of the *affinity* of the ligand towards the active site. A calculation of solvation energy (docking energy) is not required; this quantity demands heavy computing. The data reported here can eventually be used in connection with statistical mechanical methods developed by Åqvist and coworkers (see for instance [40]). However, we do not use their approach because, at this point in time, the focus is on the comparison with DOCK results and not on a methodology designed to get binding free energies. The affinity results obtained here show that the DOCK3.5 program is successful in predicting relative interaction energies (affinities). This situation prompted a docking test on a set of nitro-compounds [41] with anti-chagasic activity although they do not have in vitro specificity for the parasite enzyme.

## Methods

The docking calculations at the active sites were carried out with the crystal structures of human glutathione reductase and trypanothione reductase from *T. cruzi* [9, 13] and the available crystallographic information for the natural substrates. The program DOCK3.5 was used in all the cases reported. [35, 36] Prepared ligand molecules were docked using the contact and force field scoring scheme and subsequent output minimization. The filtering and analysis of output data were done with the o6.1 program [37] taking into account the best force field scores and the orientation of ligands with respect to the redox active group, i.e., the disulfide bridge at the G-site.

The crystal structures for the complexes GR–GSSG and TR–$T[S]_2$, along with the theoretical docking conformation of GSSG in TR, were used to seed the molecular dynamics (MD) simulations. For $T[S]_2$ in GR, the starting point came from a graphical docking since DOCK could not position the ligand properly at the corresponding site (see below). (Systems for the free (unbound) substrates were also studied.)

All MD simulations, performed with the program GROMOS87, [38] were carried out with spherical systems of 28 Å radius, centered on the ligand disulfide bridge. Water was added to fill the spheres using the SPC (simple point charge) potential in all cases. For the complexes, spheres comprised some 3,500 solute atoms and nearly 1,500 water molecules while there were as many as 3,000 solvent molecules for the unbound ligand spheres. All protein atoms and/or water molecules outside a radius of 13 Å were fixed (extended wall region method). The twin range scheme was used to treat the non-bonded interactions; van der Waals and electrostatic interactions were evaluated at every time step within a 10 Å shell. Electrostatic interactions alone were updated every 50 time steps for those atoms in the spherical shell found between 10 Å and 15 Å. Prior to the MD simulation itself, each system was energy minimized using the "steepest descent" algorithm to allow relaxation of the solvent molecules. The system was coupled to a heat bath [39] with $\tau$=0.05 where the simulation temperature was held at 300 K except during the initial heating phase when the temperature was slowly raised in steps by a 20 ps scheme. During this phase, solute atoms were restrained to their initial positions by strong harmonic restraints, which were successively weakened and finally removed at the end of the scheme. Trajectories (extended wall mode) were continued for an additional 250 ps. Non-bonded energy data were collected throughout the last 50 ps. The SHAKE algorithm was enabled to speed up simulations. Structure and energy data from the simulations were processed with the NICE package. [42]

Molecular surface and volume for $T[S]_2$ and GSSG, and the enzyme active sites, were obtained by means of GRASP. [43]

## Results

In Table 1, the GROMOS and DOCK results for the non-bonded interaction energy (total, electrostatic and van

**Table 1** DOCK and GROMOS electrostatic (el), van der Waals (vdw) and total (el plus vdw) non-bonded energies of $T[S]_2$ and GSSG docked at trypanothione reductase and glutathione reductase active sites. Output for the non-bound substrates is also included. For the docking results, energies correspond to the best score orientation which is also the closest to the redox active disulfide bridge (see Table 4). MD results represent averages over the last 50 ps of the simulations (standard deviations are given). Values in kcal $mol^{-1}$

| System | Energy | | | | | | | | | | | |
|---|---|---|---|---|---|---|---|---|---|---|---|---|
| | Molecular dynamics | | | | | | | | | Docking | | |
| | Solute–protein | | | Solute–solvent | | | Solute–protein+solute–solvent | | | el | vdw | Total |
| | el | vdw | Total | el | vdw | Total | el | vdw | Total | | | |
| GSSG | – | – | – | –537±20 | –4±1 | –541±21 | –537±20 | –4±1 | –541±21 | – | – | – |
| $T[S]_2$ | – | – | – | –401±15 | –21±4 | –422±19 | –401±15 | –21±4 | –422±19 | – | – | – |
| GR–GSSG | –414±18 | –49±4 | –463±22 | –193±12 | 10±2 | –183±14 | –607±30 | –39±6 | –646±36 | –43 | –31 | –74 |
| TR–$T[S]_2$ | –321±18 | –58±4 | –379±22 | –243±12 | 3±1 | –240±13 | –563±30 | –56±5 | –619±35 | –12 | –38 | –50 |
| GR–$T[S]_2$ | –224±17 | –75±5 | –299±22 | –84±9 | –3±1 | –87±10 | –308±26 | –78±6 | –386±32 | –8 | –13 | –21 |
| TR–GSSG | 129±20 | –48±3 | 81±23 | –372±12 | 14±2 | –358±14 | –243±32 | –34±5 | –277±37 | 2 | –25 | –23 |

der Waals contributions) are shown for GSSG and $T[S]_2$ at the active sites of GR and TR. GROMOS energies for the free solvated substrates are also included. DOCK values correspond to the best score orientations, which are also the closest to the enzyme disulfide bridge in each case. MD values represent time averages over the last 50 ps of simulation. Table 2 includes information on active sites molecular surfaces and volumes. Table 3 displays the docking and MD energies of some $T[S]_2$ molecular fragments. The distances between the sulfur atoms, one in the (rigid) docked molecule and the other from the active site disulfide, can be found in Table 4. We include in this table the distances from the nitrogen atom of the synthetic compounds (**1**) to (**4**) (shown in Scheme 2, see the Discussion section) to the proximal catalytic sulfur. Finally, Table 5 includes DOCK non-bonded interaction energy results for compounds (**1**) to (**4**).

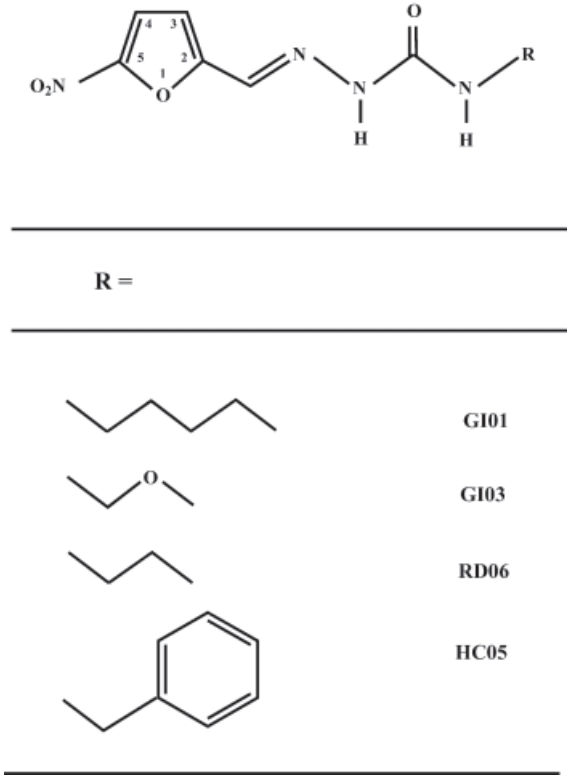


**Scheme 2** Synthesized 5-nitrofuranic derivatives

**Table 2** Solvent accessible areas (Sas) and volumes of $T[S]_2$ and GSSG. Enzyme active sites volumes are also included. Values in $Å^2$ (Sas) and $Å^3$ (volume)

| Compound | Sas | Volume |
|---|---|---|
| GSSG | 511.5 | 520.4 |
| $T[S]_2$ | 561.6 | 636.3 |
| GR active site | 1917.0 | 2422.5 |
| TR active site | 2193.3 | 2608.1 |

**Table 4** Geometric distance of closest conformation of the natural substrates and synthetic compounds to the redox active moieties of trypanohione reductase and glutathione reductase (i.e. $S_{53}$ and $S_{58}$ respectively). Data were measured from the disulfide bridge ($S_l$) in the natural substrates and the nitro group in the synthetic compounds. Values in Å

| Distance | |
|---|---|
| GR | TR |
| 4.0 | 4.1 |
| 18.0 | 5.2 |
| 4.1 | 5.6 |
| 4.0 | 5.9 |
| 4.1 | 5.8 |
| 6.2 | 5.4 |

**Table 5** Electrostatic (el), van der Waals (vdw) and total (el plus vdw) non-bonded energies of ligands docked at glutathione reductase and trypanothione reductase active sites. Energies correspond to the docked conformation closest to the redox active site disulfide bridge, respectively (see Table 4). Values in kcal $mol^{-1}$

| Compound | Energy | | | | | |
|---|---|---|---|---|---|---|
| | GR active site | | | TR active site | | |
| | el | vdw | Total | el | vdw | Total |
| GI01 (1) | –2.1 | –26.6 | –28.7 | –1.7 | –21.3 | –23.0 |
| GI03 (2) | –2.3 | –25.1 | –27.4 | –1.6 | –21.5 | –23.1 |
| RD06 (3) | –1.0 | –26.4 | –27.4 | –1.2 | –22.1 | –23.3 |
| HC05 (4) | –4.9 | –23.6 | –28.5 | –1.4 | –22.0 | –23.4 |

**Table 3** DOCK and GROMOS electrostatic (el), van der Waals (vdw) and total (el plus vdw) non-bonded energies of various $T(S)_2$ fragments docked at trypanothione reductase active site. Sper=spermidine, cys=cysteine, gly=glycine. Values in kcal $mol^{-1}$. MD values are shown in parentheses and correspond to the final output of simulation

| Fragment | Energy | | | Weighted energy[a] | | |
|---|---|---|---|---|---|---|
| | el | vdw | Total | el | vdw | Total |
| sper | –9.7 (–144) | –12.9 (–34) | –22.6 (–178) | –1.0 (–14.4) | –1.3 (–3.4) | –2.3 (–17.8) |
| gly–sper–gly | –8.9 (–174) | –15.7 (–23) | –24.6 (–197) | –0.6 (–9.7) | –1.0 (–1.3) | –1.6 (–11.0) |
| cys–gly–sper–gly–cys | –7.4 (–181) | –21.7 (–42) | –29.1 (–223) | –0.3 (–6.0) | –0.6 (–1.4) | –0.9 (–7.4) |
| $T[S]_2$ | –11.7 (–330) | –38.3 (–58) | –50.0 (–388) | –0.2 (–6.9) | –0.8 (–1.2) | –1.0 (–8.1) |

[a] Energy/number of heavy atoms in moiety

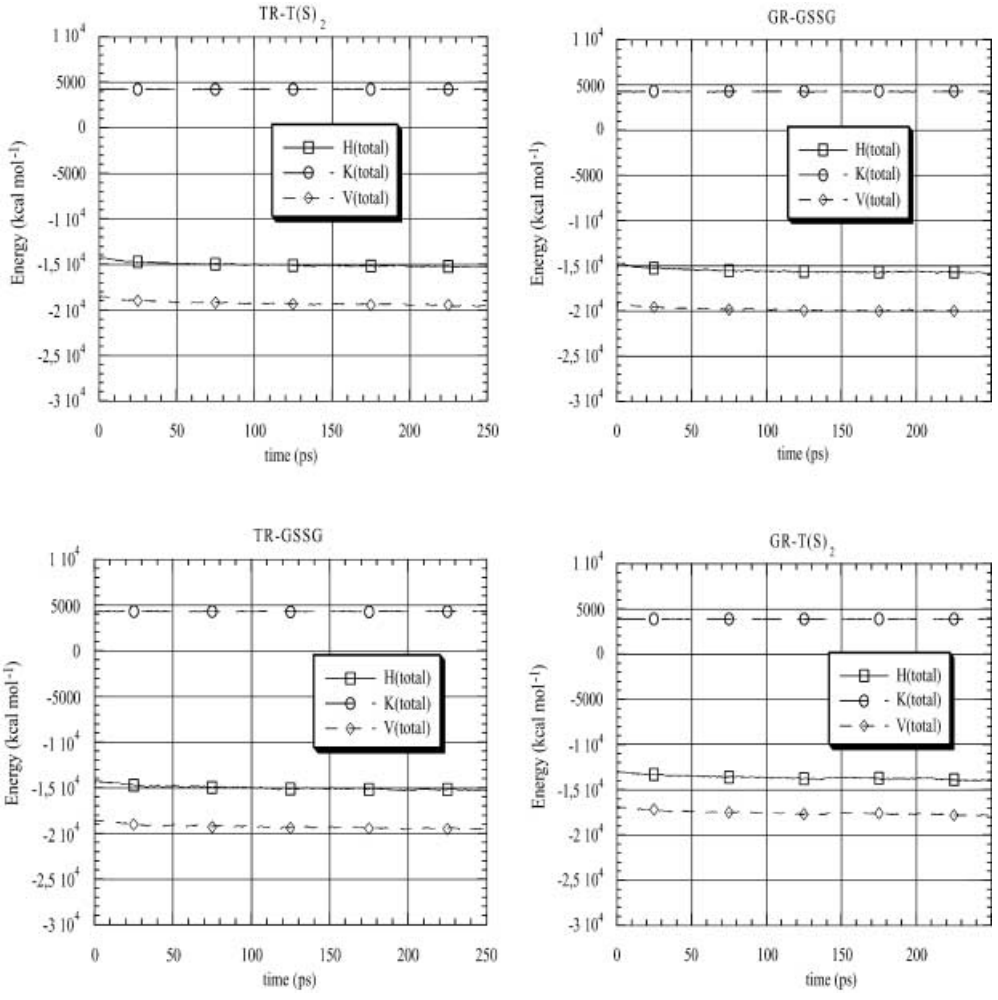


**Fig. 1** Energy results in kcal mol$^{-1}$ for the complexes TR–T[S]$_2$ and GR–GSSG, and the corresponding crossed complexes TR–GSSG and GR–T[S]$_2$, along 250 ps of MD simulation. Data from the preliminary heating phase are not included. For all cases, values are given for the whole solvated system. *V*(total)=potential energy, *K*(total)=kinetic energy, *H*(total)=total energy (*V*+*K*)

Figures 1, 2 and 3 report an analysis of the MD trajectories where overall energy and structure time evolutions are monitored, respectively. Both the energy measures and the root mean square deviations (RMSD, see Appendix 2) show that the systems attain equilibrium early. These results show the starting solvated systems were reasonably well constructed. The output from the heating step prior to the MD run is not included in the analysis. Since the motion of all solute atoms was restricted during this stage, the energetic and structural properties are not fully comparable to those of the full dynamics run (see the Methods section for more details).

The energy results derived from the docking study must be treated with caution. It is well known that energy values calculated with Molecular Mechanics strongly depend on the size (number and type of atoms) of each particular molecule and the functional form or parameterization of the force field. Thus, absolute energy values are meaningless, the discussion is restricted to energy differences between bound and free states of a ligand or with respect to two or more different receptor sites. This type of theoretical method only provides information on relative ligand affinities. On the other hand, the molecular dynamics approach is much more accurate than the scoring methods, such as DOCK itself. Because of their intrinsic static nature, DOCK results lack accessible configurational space contributions (represented by the conformational space sampling in MD); hence the docking values should be pictured as plain potentials. In addition, MD allows for an explicit treatment of the solvent, e.g. water, thus providing a closer representation of reality. The comparison between the two methods is limited to relative affinities. Therefore, no attempt is made here to calculate a docking (binding) energy; such a quantity requires supplemental information (new MD simulations of the protein in water without ligands). For this reason, the solvent–solvent energy is not reported. The energy entries are then to be used to estimate active site affinities that are comparable with those obtained with the DOCK program.

During the physiological catalytic reaction occurring in GR and TR, it is accepted that a charge transfer complex, involving the proximal sulfur atom of the enzyme disulfide ($S_{53}$ in the crystal of TR and $S_{58}$ in the crystal of GR) and $S_I$ in the disulfide substrate, forms. Figure 4 shows the orientations of GSSG in the active site of GR both as in the crystal complex and as a result of the docking (best score conformation, see Tables 1 and 4). The same information for T[S]$_2$ in TR is depicted in Fig. 5. The RMSDs of 0.3 Å and 0.9 Å between the said

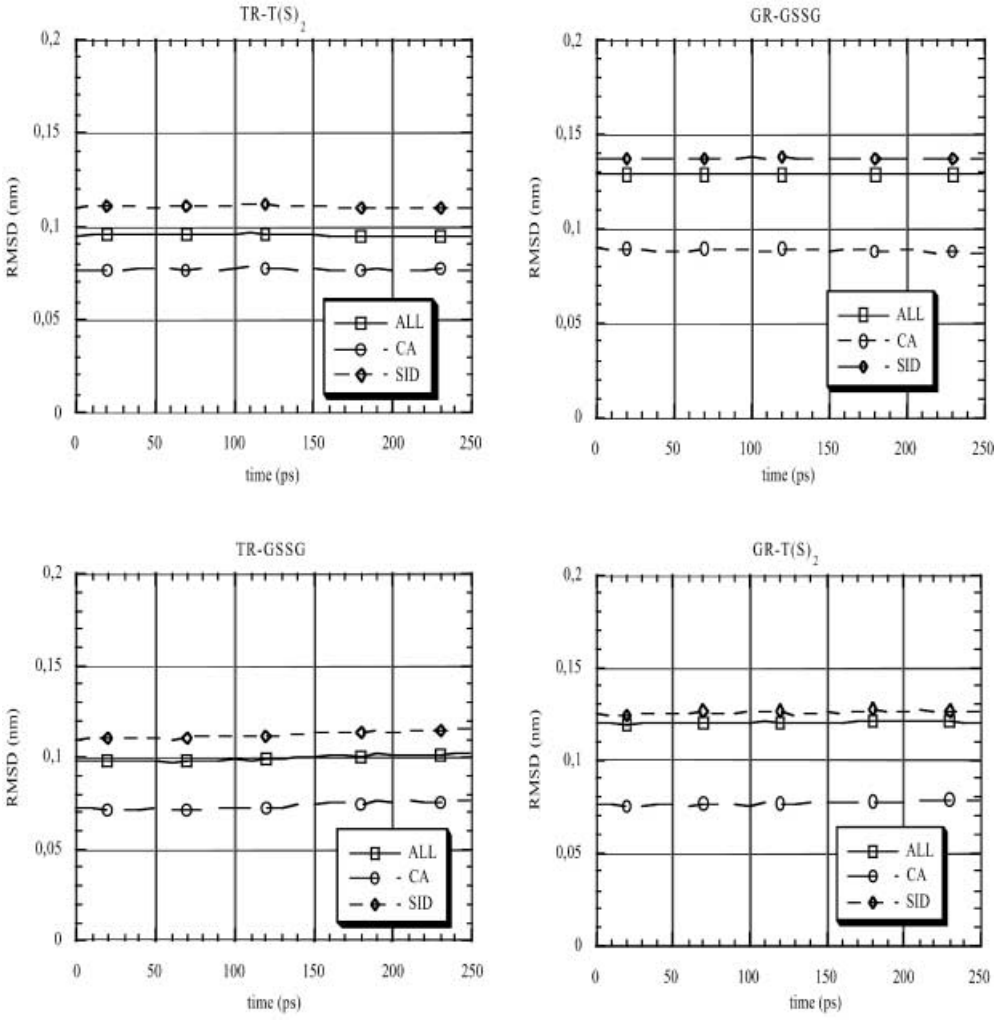


**Fig. 2** Potential energy results in kcal mol$^{-1}$ for the complexes TR–T[S]$_2$ and GR–GSSG, and the corresponding crossed complexes TR–GSSG and GR–T[S]$_2$, along 250 ps of MD simulation. Data from the preliminary heating phase are not included. For all cases, values are given for the solute (protein+ligand). *V*(total)=total potential energy, *V*(ang)=angle energy, *V*(died)=dihedral energy, *V*(imp)=improper dihedral energy, *V*(el)=electrostatic energy, *V*(vdw)=van der Waals energy

orientations of GSSG and T[S]$_2$, respectively, are evidence of the quality of the docking results compared to the experimental data, thus supporting the theoretical procedure followed here. Note, however, that the final position assigned to T[S]$_2$ in TR is not as accurate as compared with the docking of GSSG in GR. The latter is virtually the same as the experimental data.

The docking results in Table 1 (columns 11, 12 and 13) show the substrate–protein interaction energies in the crossed complexes to be well above (less stabilization) those for the natural complexes; the energies for the former are three (GSSG) and two (T[S]$_2$) times larger than the latter. For GSSG, in particular, it is apparent that the electrostatic potential varies quite a lot when bound to GR or TR (see the entry in Table 1, column 11). This, indeed, is the major component for the energy discrepancy and indicates that the electrostatic factor is dominant as far as selectivity is concerned. In fact, the natural substrates possess different electrostatic traits: GSSG carries a negative net charge (–2) and T[S]$_2$ has a positive charge of +1. This is due to the replacement of the glycine's carboxylate groups in GSSG by the amide linkage with the protonated spermidine arm in T[S]$_2$ (see Scheme 1). Accordingly, the GR active site is rich in basic residues, while in TR, neutral and acid residues prevail. Therefore, the result obtained confirms the simple electrostatic expectation.

The simulations support the docking results with respect to the relative affinities of GSSG and T[S]$_2$ to GR and TR, the crossed complexes again displaying interaction energies above those of the cognate couples (compare columns 2, 3 and 4 with 11, 12 and 13, respectively, in Table 1). In an even more marked fashion, the difference in electrostatic energies between the natural and crossed complexes is substantial (Table 1, column 2). The only disagreement occurs with the van der Waals contributions for the crossed complexes. In this context, the distances in Table 4 indicate that the spatial position assigned to GSSG by DOCK3.5 is very similar in GR and TR. For trypanothione, on the contrary, the parasite ligand ends up at very different positions: near the enzyme disulfide in TR (5 Å), but far away (18 Å) in the human enzyme. In fact, T[S]$_2$ is barely docked inside the active site of GR. This remarkable outcome clearly suggests that there is an important steric hindrance for T[S]$_2$ to accommodate at the active site of the human enzyme, hence the rather low value for

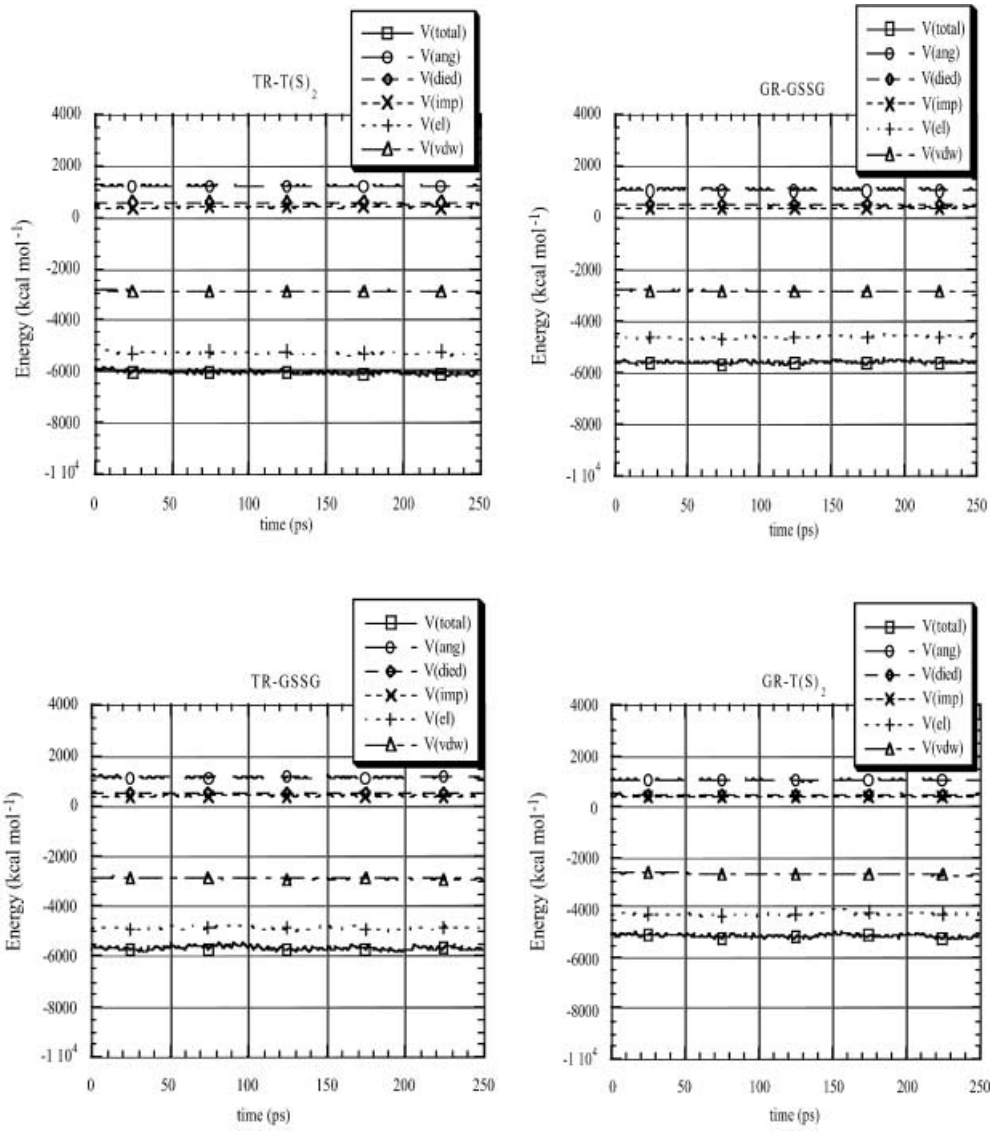


**Fig. 3** Root mean square deviations (RMSDs) in nanometers for the complexes TR–$T[S]_2$ and GR–GSSG, and the corresponding crossed complexes TR–GSSG and GR–$T[S]_2$, along 250 ps of MD simulation. For each complex, the initial optimized structure was taken as reference to calculate the geometric deviations. Data from the preliminary heating phase are not included. ALL=all atoms, CA=Cα atoms, SID=side chain atoms

the van der Waals contribution to the interaction energy of this substrate in GR. This could also suggest that DOCK3.5 encounters some difficulties when trying to adjust large substrates, e.g. $T[S]_2$, in rather narrow molecular cavities such as the GR active site. Remember that, not without considerable graphical effort, we were able to adjust $T[S]_2$ at GR and use the resulting complex as a seed for the MD trajectory (see the Methods section).

The steric factor, then, should be also taken into account when analyzing substrate specificity. This idea is further supported by the information on molecular surfaces and volumes presented in Table 2. In effect, the TR active site is some 180 $Å^3$ larger than the corresponding site in GR. This is in agreement with the size difference between the natural substrates, $T[S]_2$ and GSSG (see also Table 2). It is clear then that the parasite enzyme is designed to make the entry of larger groups easier. In the same vein, Marsh and Bradley [44] concluded that the access to the active site of TR by large aromatic groups seems to be tolerated readily.

The solvent–ligand energy interaction in Table 1 further attests to this idea (see columns 5–7 therein). In particular, for the electrostatic contribution (which represents almost exclusively the total solvent–ligand interaction for all four complexes), it is apparent that the energy values are in agreement with the number of water molecules in the neighborhood of the substrates at the active site. In the case of the TR–GSSG complex, where solvent molecules easily accommodate at the ligand's whereabouts, the value for the interaction reaches its maximum. In contrast, the lowest contribution takes place in the GR–$T[S]_2$ complex where the scenario is quite the opposite; this time the ligand displaces the solvent molecules as it fills the active site cavity.

Active site interaction energies (affinities) can be obtained readily by subtracting the non-bonded ligand–solvent energy of the free substrate system from the total (substrate–enzyme plus substrate–solvent) non-bonded energy of the corresponding complex. This can be seen from the entries in columns 8, 9 and 10 from Table 1.

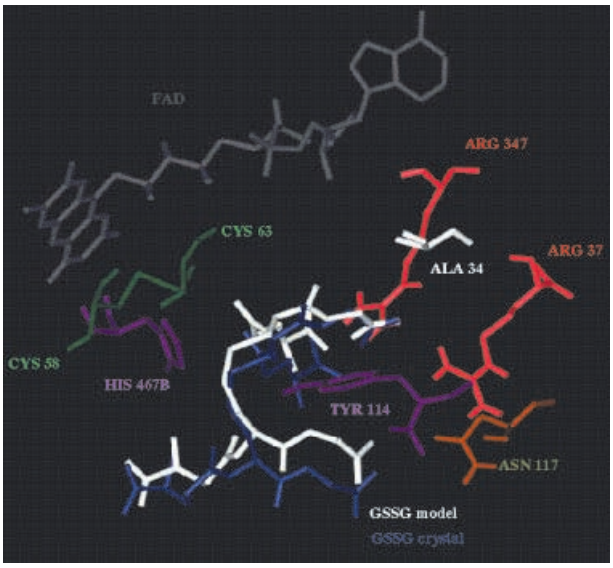


**Fig. 4** GSSG in complex with GR as in the crystal structure (*light colored*) and according to DOCK3.5 (*dark colored*). Some neighbor residues defining the active site are also included. Hydrogen atoms are not shown for the sake of clarity

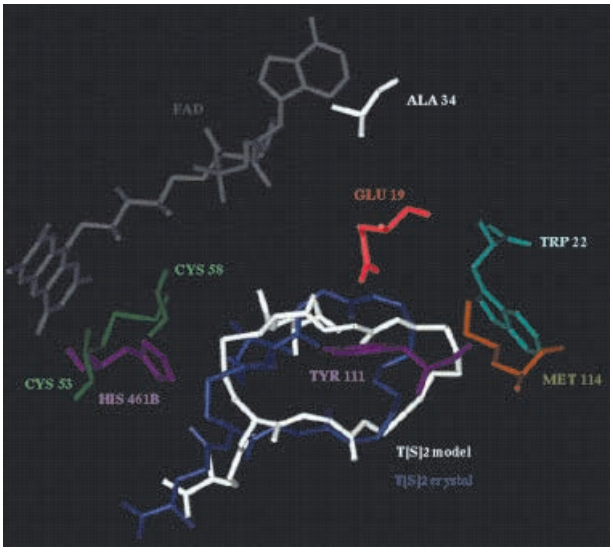


**Fig. 5** $T[S]_2$ in complex with TR as in the crystal structure (*light colored*) and according to DOCK3.5 (*dark colored*). Some neighbor residues defining the active site are also included. Hydrogen atoms are not shown for the sake of clarity

**Scheme 3** $T[S]_2$ molecular fragments. Spe=spermidine, cys=cysteine, gly=glycine, $E$=binding energy of fragment, $E_w$=$E$/number of heavy atoms in fragment

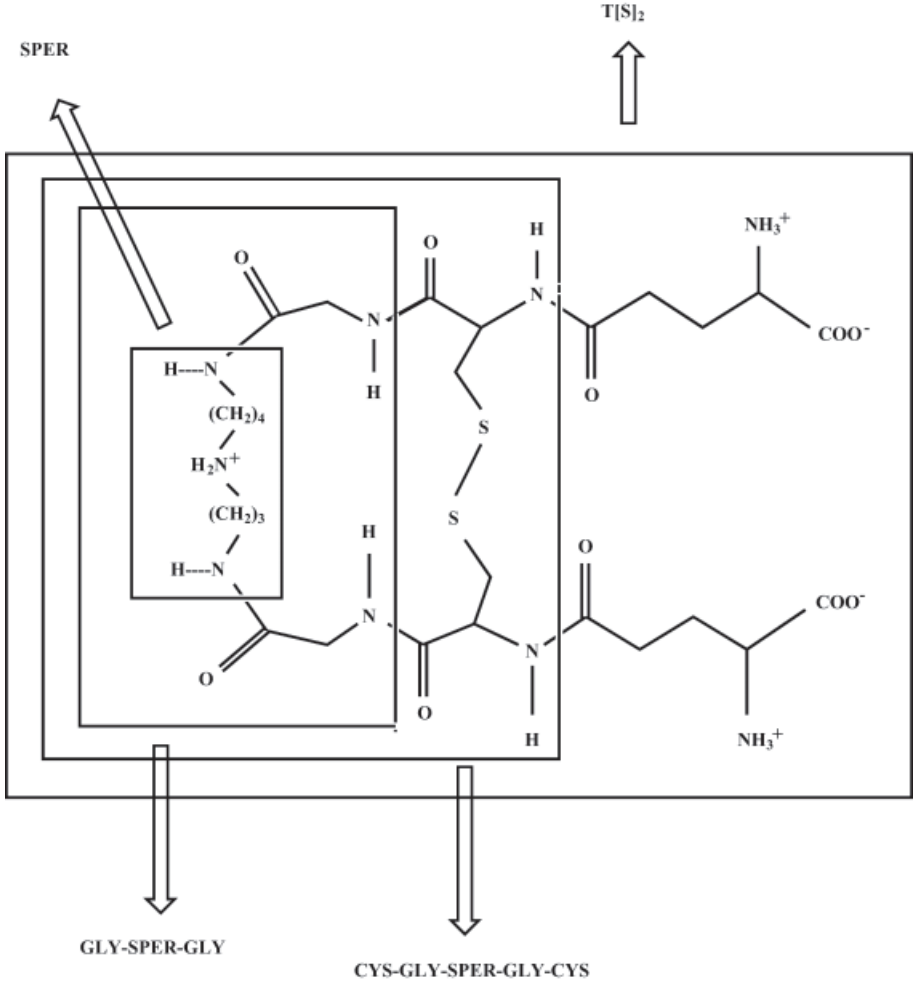

Result: the relative affinity energies of GSSG and $T[S]_2$ to the GR and TR active sites follow a similar trend to that verified when considering the interaction (non-bonded) energies of the substrate–enzyme complexes alone, namely, the physiological complexes are far more stable than the crossed pairs. The corollary is that the rigid and solvent void DOCK3.5 calculations can be taken to reproduce relative affinity energies of substrates towards different receptors' sites approximately.

The results reported in Table 3 give evidence for the crucial role of the spermidine arm in $T[S]_2$. In effect, we were able to demonstrate that it is indeed the substrate moiety that proportionally contributes the most (i.e. interaction energy averaged over the number of heavy atoms) to binding in TR (compare the results in Table 3 for different fragments of $T[S]_2$). The agreement between DOCK and GROMOS trends is striking here. The structure of the dissected $T[S]_2$ fragments is shown in more detail in Scheme 3. As the successive fragments increase in size, the averaged interaction energy systematically becomes lower, even when considering the full substrate. This must be taken into account when envisioning the design of a potential selective inhibitor of TR. In other words, this result supports the seminal notion that spermidine-like side chains should be included in the molecular design as a way to enhance the binding specificity towards the parasite enzyme. Fairlamb and coworkers [25, 26, 32] have already hinted at this idea from the experimental side.

In order to complement the energetic and structural approach, a study of molecular contacts (at less than 4.0 Å) was conducted along the MD trajectory established between the substrates and the enzyme active site residues in TR and GR. The details are not shown here. However, it is worth mentioning that they agree somewhat with the results presented herein. For the TR active site, the averaged number of contacts detected for GSSG (92) is significantly less than for $T[S]_2$ (135). In particular, contacts with key residues such as Glu15, Trp18 and Ser109 are either missing or hardly present along the simulation. On the other hand, the overall number of contacts in TR is fairly sustained for GSSG and $T[S]_2$ (156 and 160, respectively). The reason for these results becomes clear when one considers the different molecular sizes of the ligands and active sites (see above). In other words, for the crossed complexes, a smaller ligand (GSSG) is placed in a large site (TR) while a larger ligand ($T[S]_2$) is adjusted in a narrow cavity. Nevertheless, most of the contacts with the positively charged residues (Arg37 and Arg347) present in the GR–GSSG complex, are absent in the GR–$T[S]_2$ complex. This accounts for the rather low electrostatic contribution to the interaction energy in the latter (see Table 1, column 2).

## Discussion

In the literature, the mutually exclusive substrate specificity displayed by GR and TR has been ascribed to a proper balance between steric and electrostatic effects, which would optimize substrate binding at the corresponding active site. [9, 10, 12, 13, 18, 44, 45] The results presented here agree with these hypotheses. However, there is a factor not considered so far: the energy required to mold the substrates GSSG and $T[S]_2$ from their minimal energy conformation to the form adapted to the shape of the active site. Observe that the large negative interaction energy of these substrates will be compensated by the (positive) molding energy. Molecular Mechanics (MM) calculations yield +42 kcal $mol^{-1}$ of the molding energy for GSSG; using DOCK3.5 values, the GR–GSSG complex will have about –32 kcal $mol^{-1}$ (–74+42), and the complex TR–GSSG becomes unstable (+19 kcal $mol^{-1}$). For trypanothione, MM calculations give a molding energy of about +10 kcal $mol^{-1}$. Then, docking $T[S]_2$ to TR leads to –40 kcal $mol^{-1}$ stabilization energy as opposed to –11 kcal $mol^{-1}$ when docked at GR. The cross-complex TR–GSSG would not only have the smallest binding energy but in fact would be unstable. This is, of course, a simulation of the molding effect, but might well illustrate the role of this factor in actual situations.

The electrostatic nature of a given inhibitor is indeed a key feature to attain selectivity. It follows that an appropriate inhibitor should carry a positive net charge, preferably within a spermidine-like side chain, as a way to mimic the real substrate. This would favor docking in the parasite enzyme. On the other hand, the presence of a massive functional group (certainly larger than the substitutes previously studied) would be necessary to confer more binding affinity to the putative active site of TR. Thus, a truly selective inhibitor should not be able to enter the active site of GR. This is shown by the docking result of $T[S]_2$ in the glutathione reductase active site. Although these are not new notions, to the best of our knowledge, there has not been previous work where quantitative or semi-quantitative theoretical measures were presented to rationalize this idea for these systems.

DOCK3.5 and molecular dynamics results are consistent. Although, in the long run, this type of scoring methods cannot substitute for the more complex and accurate dynamics schemes, the work presented here supports DOCK3.5 as a powerful tool for reasonably and rapidly assessing the selectivity of theoretically designed potential drugs towards particular active sites or receptors.

It is, therefore, interesting to use the docking facility to study other molecules that might have potential anti-chagasic action. In fact, potential inhibitor molecules have been reported recently. [41] They are four nitrofuranic molecules where the residue -(5-nitrofurfurilidene)semi-carbazide is bound to the functional groups 4-hexyl-1-, 4-(2-methoxyethyl)-1-, 4-butyl-1-, and (2-phenylethyl)-1-, respectively. These molecules were designated by the symbols GI01 (**1**), GI03 (**2**), RD06 (**3**) and HC05 (**4**) in the original paper. [41] In Scheme 2 their chemical formulae are depicted. Their docking suggests that orientations where the nitro group

can interact with the active disulfide bridge of both TR and GR are easily accessible (see Table 4). The interaction energy found there is reported in Table 5. The results indicate that these nitro compounds would form more stable complexes in GR than in TR putative active G-sites. Furthermore, the molding work for these compounds is probably independent of the differences in active sites because there is plenty of room there. From the numbers in Table 5, one may expect a better binding to GR than to TR. In a recent study from our laboratory, [46] a marginal preference (in vitro) of these compounds for the human enzyme was found. It is apparent that these compounds have poor specificity for the TR enzyme. None of them has a positive charge center in its structure. The agreement found between DOCK3.5 and the experiments is therefore a rewarding result. To conclude, the results discussed here can be used as a validation test to use this method in designing anti-chagasic ligands.

**Acknowledgments** F.I. thanks PEDECIBA-Química for financial support. M.P. thanks the SAREC/SIDA program for continued financial support. S.A. and M.M. thank the Regional Government of the II Region, Antofagasta and Minera Escondida Ltda. for their financial assistance. O.T. thanks NFR (Swedish Research Council) for sustained financial support.

## Appendix 1. Force field scoring in DOCK3.5

Force field scores are approximate molecular mechanics interaction energies, consisting of van der Waals and electrostatic components:

$$E = \sum_{i=1}^{\text{lig}} \sum_{j=1}^{\text{rec}} \left[ \frac{A_{ij}}{r_{ij}^{12}} - \frac{B_{ij}}{r_{ij}^{6}} + 332.0 \frac{q_i q_j}{D r_{ij}} \right] \quad (1)$$

The double sum is over ligand (lig) and receptor (rec) atoms. The coefficients $A_{ij}$ and $B_{ij}$ are the van der Waals repulsion and attraction parameters; $r_{ij}$ is the distance between atoms $i$ and $j$; $q_i$ and $q_j$ are the point charges on atoms $i$ and $j$. $D$ is a dielectric function. The numeric factor is needed to convert the energy into kcal mol$^{-1}$.

DOCK 3.5 performs a grid calculation using a geometric mean approximation for the van der Waals parameters:

$$A_{ij} = \sqrt{A_{ii}\sqrt{A_{jj}}} \text{ and } B_{ij} = \sqrt{B_{ii}\sqrt{B_{jj}}} \quad (2)$$

The single-atom-type parameters are derived from the van der Waals radius, $R$ and well depth, ε, according to:

$$A = \varepsilon [2R]^{12} \text{ and } B = 2\varepsilon [2R]^{6} \quad (3)$$

The ligand–receptor interaction energies are calculated for every grid point in the particular molecular surface. A more in-depth description of the calculation procedure can be found in. [47, 48]

The Gromos force field [38, 39] includes standard contributions:

$$V = V_{\text{bond}} + V_{\text{bend}} + V_{\text{imp-dih}} + V_{\text{tor}} + V_{\text{LJ}} + V_{\text{elec}} \quad (4)$$

$V_{\text{bond}}$, $V_{\text{bend}}$, and $V_{\text{imp-dih}}$ are the harmonic potentials for bond vibrations, bendings, and improper dihedral motions, respectively; the $V_{\text{tor}}$ term corresponds to dihedral torsions. These short-range potentials in Eq. (4) arose in the 1930s for the quantitative analysis of molecular infrared spectra. The improper dihedral potential corrects for the fact that the α-carbon effective atom model does not include explicitly the corresponding hydrogen. The last two terms in Eq. (4) correspond to the nonbonded pair potential (or van der Waals potential, modeled by a Lennard-Jones 6–12 function), and the electrostatic interaction between point charges, respectively. In the model used for protein in water, protonated groups have net positive charge, while carboxylated groups may have a net negative charge depending upon pH. For instance, at low pH, a protein may have all lysine, histidine, and arginine groups protonated, while aspartic and glutamic residues remain neutral.

Dock and Gromos potential functions share the $V_{\text{LJ}}+V_{\text{elec}}$ terms, although the actual parameters differ. Comparisons of trends are then meaningful.

## Appendix 2. Root mean square deviations

Root mean square deviations (RMSDs) for one or a set of structures (i.e. during an MD simulation) with respect to a reference structure, can be calculated using the formula: [49]

$$\text{RMSD} = \sqrt{\frac{\sum_{i=1}^{N} \left[ (X_i - X_{i,\text{ref}})^2 + (Y_i - Y_{i,\text{ref}})^2 + (Z_i - Z_{i,\text{ref}})^2 \right]}{3N}} \quad (5)$$

where $N$ is the number of atoms, $X_i$, $Y_i$ and $Z_i$ are the coordinates of atom $i$ from a particular structure and $X_{i,\text{ref}}$, $Y_{i,\text{ref}}$ and $Z_{i,\text{ref}}$ the coordinates of atom $i$ in the reference structure.

## References

1. Moncayo A (1993) In: Tropical disease research; progress 1991–1992. World Health Organization, Geneva, pp 67–72
2. deCastro S (1993) Acta Trop 53:83–98
3. Schirmer RH, Muller JG, Krauth-Siegel RL (1995) Angew Chem Int Ed Engl 34:141–154
4. Verlinde CLMJ (1994) Structure 2:577–587
5. Hunter WN, Bailey S, Habash J, Harrop SJ, Helliwell JR, Aboagye-Kwarteng T, Smith K, Fairlamb AH (1992) J Mol Biol 227:322–333
6. Fairlamb AH (1999) Medicina 59:179–187
7. Fairlamb AH, Cerami A (1992) Annu Rev Microbiol 46:695–729
8. Karplus PA, Schulz GE (1989) J Mol Biol 210:163–180
9. Mittl PRE, Schulz GE (1994) Protein Sci 3:799–809
10. Lantwin CB, Schlichting I, Kabsch W, Pai EF, Krauth-Siegel RL (1994) Proteins 18:161–173
11. Zhang Y, Bond CS, Bailey S, Cunningham ML, Fairlamb AH, Hunter WN (1996) Protein Sci 5:52–61
12. Bailey S, Smith K, Fairlamb AH, Hunter WN (1993) Eur J Biochem 213:67–75

13. Bond CS, Zhang Y, Berriman M, Cunningham ML, Fairlamb AH, Hunter WN (1999) Structure 7:81–89
14. Shames SL, Fairlamb AH, Cerami A, Walsh CT (1986) Biochemistry 25:3519–3526
15. Krauth-Siegel RL, Enders B, Henderson GB, Fairlamb AH, Schirmer RH (1987) Eur J Biochem 164:123–128
16. Ghisla SK, Massey V (1989) Eur J Biochem 181:1–17
17. Schirmer RH, Krauth-Siegel RL, Schulz GE (1989) In: Dolphin P, Poulson R, Avramovic O (eds) Glutathione: chemical, biochemical and medical aspects, part A. Wiley, New York, pp 553–596
18. Hunter WN, Smith K, Derewenda Z, Harrop SJ, Habash J, Islam MS, Helliwell JR. Fairlamb AH (1990) J Mol Biol 216:235–237
19. Karplus PA, Pai EF, Schulz GE (1989) Eur J Biochem 178:693–703
20. Diaz W, Aullo JM, Paulino M, Tapia O (1996) Chem Phys 204:195–203
21. Iribarne F, Paulino M, Tapia O (2000) Theor Chem Acc 103:451–462
22. Henderson GB, Fairlamb AH, Ulrich P, Cerami A (1987) Biochemistry 26:3023–3027
23. Dumas C, Ouelette M, Tovar J, Cunningham ML, Fairlamb AH, Tamar S, Olivier M, Papadopoulou B (1997) EMBO J 16:2590–2598
24. Tovar J, Cunningham ML, Smith AC, Croft SL, Fairlamb AH (1998) Proc Natl Acad Sci USA 95:5311–5316
25. Tovar J, Wilkinson S, Mottram JC, Fairlamb AH (1998) Mol Microbiol 29:653–660
26. Henderson GB, Ulrich P, Fairlamb AH, Rosenberg I, Pereira M, Sela M, Cerami A (1988) Proc Natl Acad Sci USA 85:5374–5378
27. Jockers-Scherubl MC, Schirmer RH, Krauth-Siegel LR (1989) Eur J Biochem 180:267–272
28. Mester B, Hikichi N, Hansz M, Paulino M (1990) Chromatographia 30:191–194
29. Benson TJ, McKie JH, Garforth J, Borges A, Fairlamb AH, Douglas KT (1992) Biochem J 286:9–11
30. Cunningham ML, Zvelebil MJJM, Fairlamb AH (1994) Eur J Biochem 221:285–295
31. Jacoby EM, Schlichting I, Lantwin CB, Kabsch W, Krauth-Siegel RL (1996) PROTEINS 24:73–80
32. Chan C, Yin H, Garforth J, McKie JH, Jaouhari R, Speers P, Douglas KT, Rock PJ, Yardley V, Croft SL, Fairlamb AH (1998) J Med Chem 41:148–156
33. Stoppani AOM (1999) Medicina 59:147–165
34. Tapia O, Paulino M, Stamato FMLG (1994) Mol Eng 3:377–414
35. Kuntz ID (1992) Science 257:1078–1082
36. Kuntz ID, Meng EC, Shoichet BK (1994) Acc Chem Res 27:117–123
37. Jones TA, Kjeldgaard M (1990) Manual for O. Uppsala University
38. van Gunsteren WF, Berendsen HJC (1987) Groningen Molecular Simulation (GROMOS) Library Manual. Biomos, Groningen, The Netherlands
39. Berendsen HJC, Postma JPM, Di Nola A, van Gunsteren WF, Haak HR (1984) J Chem Phys 81:3684–3690
40. Åqvist J, Hansson T (1996) J Phys Chem 100:9512–9521
41. Cerecetto H, Di Maio R, Ibarruri G, Seoane G, Denicola A, Quijano C, Peluffo G, Paulino M (1998) Il Farmaco 53:89–94
42. Nilsson O (1990) J Mol Graph 8:192–200
43. Nicholls A, Sharp K, Honig B (1991) PROTEINS 11:281–296
44. Marsh I, Bradley M (1997) Eur J Biochem 248:690–694
45. Faerman CH, Savvide SN, Strickland C, Breidenbach MA, Ponasik JA, Ganem B, Ripoll D, Krauth-Siegel KL, Karplus PA (1996) Bioorg Med Chem 4:1247–1253
46. Paulino M. Iribarne F, Hans M, Vega M, Seoane G, Cerecetto H, Di Maio R, Caracelli I, Zukerman-Schpector J, Olea C, Stoppani AOM, Berriman M, Fairlamb AH, Tapia O (2002) J Mol Struct (Theochem) in press
47. Meng EC, Shoichet BK, Kuntz ID (1992) J Comput Chem 13:505–524
48. Meng EC, Gschwend DA, Blaney JM, Kuntz ID (1993) PROTEINS 17:266–278
49. Kenney JF, Keeping ES (1962) The standard deviation. In: Mathematics of statistics Pt. 1, 3rd edn. Van Nostrand, Princeton, N.J. pp 77–80